UNITÉ DE RECHERCHE
INRIA-SOPHIA ANTIPOLIS

Institut National
de Recherche
en Informatique
et en Automatique

2004 route des Lucioles
B.P. 93
06902 Sophia-Antipolis
France

Rapports de Recherche

N°1787

Programme 4

Robotique, Image et Vision

THE GRADIENT AND LAPLACIEN FILTERED BACK PROJECTION OPERATORS

Jean-Philippe THIRION

Novembre 1992

The Gradient and Laplacien Filtered Back Projection Operators

Jean-Philippe THIRION *
INRIA, Epidaure †

September 30, 1992

Abstract

This paper presents a new method, based on the Filtered Back Projection technique (FBP), to compute directly the values of the gradient and the laplacien of an X-Ray image. We propose a way to pre-process the raw data that allow us to compute directly the reconstructed values of the gradient or of the laplacien at any location in the plane (defined with real coordinates), without reconstructing an image of the absorption coefficients. The reconstructed values of the gradient and of the laplacien correspond to the exact mathematical definition of the differentials of the image, and do not imply the use of a band limited filter depending on a constant σ, as proposed previously by other authors. For noisy data, we propose also an extension of existing FBP techniques, adapted to the computation of the gradient and of the laplacien. At last, we show how to use those new algorithms to perform the segmentation of a slice, without image reconstruction. Images of the reconstructed gradient, laplacien and segmented objects are presented.

Key words: XRay Tomography, Filtered Back Projection, Edge detection, Gradient, Laplacien.

*Email: jean-philippe.thirion@inria.fr
†http://zenon.inria.fr:8003/Equipes/EPIDAURE-eng.html

Les opérateurs de rétro-projection filtrée gradient et laplacien

Jean-Philippe THIRION
INRIA, Epidaure

Résumé

Cet article présente une méthode entièrement nouvelle, basée sur la technique de rétro-projection filtrée (ou FBP), qui permet le calcul direct des valeurs de gradient et de laplacien d'une coupe tomographique obtenue par rayons X. Nous proposons de pré-calculer les images brutes de façon à pouvoir obtenir directement les valeurs de gradient et de laplacien en n'importe quel point de coordonnées réelles du plan de coupe, sans qu'il soit nécessaire de reconstruire une image des cœfficients d'absorption. Les valeurs que nous reconstruisons correspondent à la définition mathématique exacte des différentielles de la fonction image, et n'impliquent pas l'utilisation d'un filtre passe-bande dépendant d'une constante σ, contrairement aux méthodes proposées précédemment. Pour le cas des données bruitées, no us proposons également une extension de techniques existantes pour la rétro-projection filtrée, et adaptée cette fois au cas du gradient et du laplacien. Enfin, nous montrons comment utiliser ces nouveaux opérateurs pour éffectuer la segmentation d'une coupe, sans reconstructi on d'image et nous présentons des images de gradient et de laplacien reconstruites, ainsi que des exemples de segmentation.

Mots clef: tomographie par rayons X, rétro-projection filtrée, détection de contour, gradient, laplacien.

1 Introduction

In the past decade, most work in the Medical Image Processing field was centered on producing high quality images, mainly for diagnostic and visualization. For X-ray scanner images (cat-scan), many techniques have been proposed to transform the raw data produced by the scanner, called sinogram, into an image representing a slice of the patient. Three main types of techniques have emerged, classified into Algebraic, Analytic or Stochastic reconstruction methods. Then, other Image Processing Methods, generally refered to as *segmentation methods*, have been proposed to extract high level information from those images, such as the edge or the surface boundaries of the scanned objects. Few works have been proposed to extract directly those high level information from the raw data, which is the goal of the present paper.

We have already presented such an algorithm, called Geometric Tomography (see [12]), to perform the segmentation of the data directly in the space of the sinogram, and to convert geometrically those segmented contours into reconstructed contours in the usual space, which is the final goal. We have shown that, under the assumption that the objects are sufficiently smooth and high contrasted, real time tracking of object boundaries can be achieved, with subpixel positioning of the reconstructed surface, and with an algorithm which is linear with respect to the number of the viewing angles. In the present paper, we show a new method, this time based on the use of the gradient and/or laplacien computation, along with the Filtering Back Projection algorithm (FBP), to perform the segmentation. Both algorithms have been described for the first time in [11], for real time tracking of object boundaries.

The FBP is one of the Analytical Reconstruction method, a good introduction to this technique can be found in [5]. Srinivasa et al. (see [8]) have proposed recently a way to incorporate the differential filters, which are traditionally used to compute the gradient and the laplacien values, directly into the filter used in the Filtered Back Projection algorithm. Our own method is close to this one in that we propose modified filters to perform the Filtered Back Projection. The originality of our method is that we don't incorporate a band-limited filter depending on a constant σ, but we derive new filters based on the exact mathematical definition of the gradient and the laplacien.

For those who are not familiar with these notions, we first explain the general principles of our method, from the viewpoint of signal processing. Then we define precisely two new operators called the *Gradient Filtered Back Projection* (GFBP) and the *Laplacien Filtered Back Projection (LFBP)* operators. We show how to modify these new operators to incorporate low frequency filtering for noisy data. We provide also an efficient algorithm which use the GFBP and the LFBP to perform the segmentation of the images. At last, we show experimental results obtained with our method.

2 The principles of our method

The computation of the zero-crossing of the laplacien of an image is a traditional approach to the segmentation problem (see Marr and Hildreth [7]). Another approach to the segmentation is to compute the gradient of the image, and to define the contours to be the loci of the extrema of the norm of the gradient, in the gradient direction (see Canny [1], Deriche [2]). In this approach, which incorporates a model of the contour and a model of the noise, the method gives the optimal tradeoff with respect to the position accuracy and the noise robustness. Both methods have their own advantages; for example, the zero-crossing of the laplacien defines contours which are closed curves, but can't be used to find T junctions of edges, for which directional filters are required. Many other segmentation methods make use of the computation of the gradient and/or of the laplacien, thus it is important to have efficient and reliable algorithms to compute those values.

2.1 Traditional edge detection methods

One possibility is to compute first the reconstructed image of the slice of the object, for example with the Filtered Back Projection Algorithm, and then to use filtering techniques, based on the convolution of the digital image $f_{x,y}$ with a low-frequency continuous filter $k(x,y)$ to compute the gradient and the laplacien values. This technique is based on a well-known property of the convolution operator which states that if $\hat{f}(x,y)$ is the estimated continuous function corresponding to the convolution of f with k: $\hat{f} = f * k$, then any differential of $\hat{f}$ is the convolution of f with the corresponding differential of k. For example:

$$\frac{\partial \hat{f}}{\partial x} = f * \frac{\partial k}{\partial x} \qquad \frac{\partial \hat{f}}{\partial y} = f * \frac{\partial k}{\partial y} \tag{1}$$

$$\triangle \hat{f} = \frac{\partial^2 \hat{f}}{\partial x^2} + \frac{\partial^2 \hat{f}}{\partial y^2} = f * (\frac{\partial^2 k}{\partial x^2} + \frac{\partial^2 k}{\partial y^2}) \tag{2}$$

Where $\vec{\bigtriangledown}\hat{f} = (\partial \hat{f}/\partial x, \partial \hat{f}/\partial y)$ is the estimated gradient vector and $\triangle \hat{f}$ the estimated laplacien function of the digital image f. To understand fully the contribution of our paper, it is very important to notice that those methods compute estimated functions, which depend entirely on the convolution filter k. One generally use as function k either the gaussienne function $exp^{r^2/2\sigma^2}$, with $r^2 = x^2+y^2$, as in [7], or the function $exp^{(|x|+|y|)/\sigma}$ as in [2], or sometimes the sinus cardinal function $sinc(r/\sigma)$. σ corresponds to a smoothing factor, which is chosen being a tradeoff between the precision in the position of the contour and noise robustness. As we can see, none of those methods avoid the use of a low frequency filter, depending on a constant σ. This is why we will denote by k_σ these kind of filters.

2.2 The filtered back projection method

Filtered back projection (or FBP) is the most wide spread method of reconstruction from projections. In the following, the equations will be designed for parallel beam projections, but the same operations can be designed for fan beam projection data or for projection data with an exponential absorption of the X-rays (used for example for SPECT or PET data). The following equations summarize the process of filtered back projection (see [5] for more details):

$$f(x,y) = \int_0^\pi Q(xcos(\theta) + ysin(\theta), \theta) d\theta \tag{3}$$

$$Q(u,\theta) = \int_{-\infty}^{\infty} S(\alpha,\theta) h(u-\alpha) d\alpha \tag{4}$$

$$h(t) = \int_{-W}^{W} |w| exp^{2i\pi wt} dw \tag{5}$$

Where:

- $f(x, y)$ corresponds to the value of the absorption coefficient in the slice, at the location (x, y) in the object (or "usual") space.

- $S(u, \theta)$ is the value of the integral along the line (u, θ) of the absorption coefficient. S is also called the 2D radon transform of f. Namely, $S(u, \theta)$ is the signal received by the detector at the location u along the detector line of the X-ray scanner, when its rotation angle is θ. The collection of all these values forms a 2D image called sinogram, which is a discretized version of the radon transform S.

- W: The theory of FBP implies to set a maximum value to the frequency of the signal into the sinogram. It is supposed that beyond that frequency, the spectral energy of the signal is zero.

The principle of the Filtered Back Projection algorithm is the following: the value of the absorption coefficient for each point of the slice, $f(x, y)$, is the integral along a sinusoid of the values of an image $Q(u, \theta)$, in the space of the sinogram (equation 3). The image $Q(u, \theta)$ is the convolution of the sinogram $S(u, \theta)$, with a band limited filtering function $h(t)$ (equation 4). The filtering function $h(t)$ is given by the equation 5, which can be transformed into:

$$h(t) = \frac{W sin(2\pi W t)}{\pi t} + \frac{cos(2\pi W t) - 1}{2\pi^2 t^2} \tag{6}$$

The sinogram is sampled according both the spatial dimension u and the angular dimension θ. Therefore, if the detectors are regularly spaced with an interval of τ, the maximum frequency must be set to $W = 1/2\tau$. Equation 7 gives h for successive discrete values.

$$h(n\tau) = \begin{cases} 1/4\tau^2 & n = 0, \\ 0, & n \ is \ even, \\ -1/n^2\pi^2\tau^2 & n \ is \ odd, \end{cases} \tag{7}$$

The integral along the sinusoid for θ in $[0, \pi[$ of the function $Q(u, \theta)$ in the continuous scheme is replaced with a summation of the values of a discretized image of Q in real implementations. The position $u = xcos(\theta) + y\sin(\theta)$ is generally not an integer, therefore the corresponding value must be interpolated in the image of Q. It is important to notice that the FBP allows to compute the value of the absorption coefficient for any point of the slice

with *real* coordinates. We call the process which takes the filtered sinogram and gives back the intensity value for a couple of real coordinates the FBP *operator*. It can be used for other purpose than the computation of a digital image, and avoid the definition of a fixed sampling rate of the reconstructed image, which leads to information loss.

2.3 Incorporating derivative filters into the FBP

Using the convolution property of the radon transform, Srinivasa et al. [8] have shown a way to incorporate the filter k_σ used for the computation of the gradient and the laplacien in traditional methods directly into the filter h of the Filtered Back Projection. Mainly, they have shown that replacing the filter h of the FBP method with a filter $h_\sigma = h * e_\sigma$, where e_σ is the radon transform of the filter k_σ, leads to a modified FBP algorithm which allows the computation of laplacien values.

They have determined the equations corresponding to this filter h_σ for the case of the Marr-Hildreth operator $k_\sigma = exp^{-r^2/2\sigma^2}$, and indicated that other filters can be derived using the same scheme. The resulting filter h_σ used for back projection is then the following (from [8]):

$$e_\sigma(t) = (\frac{1}{\sqrt{2\pi}\sigma^5})(t^2 - \sigma^2)exp^{-t^2/2\sigma^2} \tag{8}$$

2.4 Direct computation of differentials with FBP

Our approach is different in that we don't try to incorporate a smoothing filter depending on a constant k_σ to the reconstruction method, but we derive mathematically the exact equations for the reconstruction of the differentials of the image function f, by differentiating the equation 3, for example:

$$\frac{\partial f}{\partial x}(x,y) = \int_0^\pi \frac{\partial Q}{\partial x}(xcos(\theta) + ysin(\theta), \theta)d\theta \tag{9}$$

In the following sections, we develop the equations for the gradient and the laplacien operators.

3 The Gradient and the Laplacien FBP operator

Let see how to compute the gradient $\vec{\bigtriangledown} f = (\partial f/\partial x, \partial f/\partial y)$ of the image function f. From equation 9 (and similarly for the y direction) we have:

$$\frac{\partial f}{\partial x}(x,y) = \int_0^{\pi} cos(\theta) Q'(xcos(\theta) + ysin(\theta), \theta) d\theta \tag{10}$$

$$\frac{\partial f}{\partial y}(x,y) = \int_0^{\pi} sin(\theta) Q'(xcos(\theta) + ysin(\theta), \theta) d\theta \tag{11}$$

With:

$$Q'(u,\theta) = \frac{\partial Q}{\partial u}(u,\theta) = \int_{-\infty}^{+\infty} S(\alpha,\theta) h'(u-\alpha) d\alpha \tag{12}$$

$$h'(t) = \frac{dh}{dt}(t) = \frac{1}{\pi^2 t^3}[(2\pi^2 W^2 t^2 - 1)cos(2\pi W t) - 2\pi W t sin(2\pi W t) + 1] \tag{13}$$

As we can see in equations 10 and 11, $\partial f/\partial x$ (respectively $\partial f/\partial y$) is the integral along a sinusoid, weighted by $cos(\theta)$ (respectively by $sin(\theta)$), of a an image $Q'(u,\theta)$. This new image $Q'(u,\theta)$ is the convolution of the sinogram $S(u,\theta)$ (equation 12) with our new filter $h'(t)$, which is simply the derivative of the filtering function $h(t)$ (equation 13). The discrete version of this filter is given by the following equations:

$$h'(n\tau) = \begin{cases} 0 & n = 0, \\ 1/2\tau^3 n, & n \ is \ even, \\ (4 - \pi^2 n^2)/(2\pi^2 \tau^3 n^3) & n \ is \ odd, \end{cases} \tag{14}$$

Let see now how to compute the laplacien $\triangle f$ of the image using the same scheme. We differentiate once more the equations 10 and 11 with respect to x and y, this gives:

$$\frac{\partial^2 f}{\partial x^2} = \int_0^{\pi} cos^2(\theta) Q''(xcos(\theta) + ysin(\theta), \theta) d\theta \tag{15}$$

$$\frac{\partial^2 f}{\partial y^2} = \int_0^{\pi} sin^2(\theta) Q''(xcos(\theta) + ysin(\theta), \theta) d\theta \tag{16}$$

Therefore, we have:

$$\triangle f = (\frac{\partial^2 f}{\partial x^2})^2 + (\frac{\partial^2 f}{\partial y^2})^2 = \int_0^{\pi} Q''(xcos(\theta) + ysin(\theta), \theta) d\theta \tag{17}$$

$$Q''(u,\theta) = \frac{\partial^2 Q}{\partial u^2}(u,\theta) = \int_{-\infty}^{+\infty} S(\alpha,\theta) h''(u-\alpha) d\alpha \tag{18}$$

$$h''(t) = \frac{d^2 h}{dt^2}(t) = -\frac{3h'(t)}{t} - \frac{4\pi W^3 sin(2\pi W t)}{t} \tag{19}$$

Therefore the laplacien is the back projection of the image $Q''(u,\theta)$ (equation 17, which is the convolution of the sinogram with $h''(t)$ (equation 18), the second derivative of the filtering function of the FBP. We give also the discrete formula for this filter:

$$h''(n\tau) = \begin{cases} -\pi^2/8\tau^4 & n = 0, \\ -3/2\tau^4 n^2, & n \ is \ even, \\ -3(4-\pi^2 n^2)/(2\pi^2\tau^4 n^4) & n \ is \ odd, \end{cases} \tag{20}$$

Except for the use of this new filters h' and h'', the other operations to perform are the same than for the FBP operator. We have named the global method of gradient reconstruction *the GFBP operator* and of laplacien reconstruction *the LFBP operator*. As for the FBP operator, the values of the gradient and of the laplacien can be computed for any individual point (x,y), where x and y are real coordinates, and there is no need to reconstruct an entire image in the usual space to apply these operators. The only requirement is to pre-process the images of Q' and of Q'' of equations 12 and 18 with 1D linear filtering.

At last, we can see that the filters h' and h'' do not depend on a smoothing factor σ as for the filter h_σ proposed by Srinivasa et al. Our method corresponds to the exact mathematical solution in the sense that, for an infinite number of projections, the exact differential values are reconstructed.

4 GFBP and LFBP for noisy data

One way to handle the problem of the noise in the Filtered Back Projection technique is to apply a low frequency filter to the sinogram before back projection. Different techniques exist, corresponding to the different kind of

functions used. The filter h of back projection is modified into $\tilde{h} = h * l$, where l is the low frequency filter. If we look at the fourier transform $\mathcal{F}(\tilde{h})$ of $\tilde{h}$, we have: $\mathcal{F}(\tilde{h}) = \mathcal{F}(h) \cdot \mathcal{F}(l)$. The representation of the function $L = \mathcal{F}(l)$ is a convenient way to define and to compute the filter $\tilde{h}$. The effect of L on the power spectrum of the signal of S is very easy to understand, and the computation of $\tilde{h}$, is given by the following formula, derived from equation 5:

$$\tilde{h}(t) = \int_{-W}^{W} L|w| exp^{2i\pi wt} dw \tag{21}$$

The same scheme can be applied to the computation of $\tilde{h}'$ and $\tilde{h}''$ which are modified versions of h' and h'' which take the noise into account.

$$\tilde{h'}(t) = \int_{-W}^{W} L2i\pi w|w| exp^{2i\pi wt} dw \tag{22}$$

$$\tilde{h''}(t) = -\int_{-W}^{W} L4\pi^2 w^2|w| exp^{2i\pi wt} dw \tag{23}$$

We have shown in figure 1 several of the L functions, sometimes called *apodisation functions*, which have been proposed (see [9],[3],[4]). We have derived the analytical solutions for the functions $L = cos(t)$ and $L = cos^2(t)$, and for the gradient and laplacien filter. For example, equation 24 is the result for the Cosine square function in the case of the laplacien filter:

$$\begin{aligned} \tilde{h''}(t) = \tfrac{1}{\pi^2 t^3 (t2-1)^3} \quad & [(\pi^2 t^6 - 2\pi^2 t^4 - 12t^4 + 6t^2 - 2 + \pi^2 t^2) cos(\pi t) + \\ & (-6\pi t^5 - 2\pi t + 8\pi t^3) sin(\pi t) + \\ & (2 - 6t^2 - 4t^6)] \end{aligned} \tag{24}$$

It would be interesting to see how this filter $\tilde{h''}$ compares with the filter h_σ proposed by Srinivasa et al., the only problem is how to set the parameter σ to perform a fair comparison between the two ? The same problem arizes if we are to compare the result of the computation of the Cosine square filtered LFBP with the application of conventional laplacien operator k_σ on a Cosine square filtered FBP image. At last, one advantage of our method is that one needs not to define the σ constant, but only to choose between the L functions the most suitable one, whose effect on the power spectrum of the image is very easy to understand.

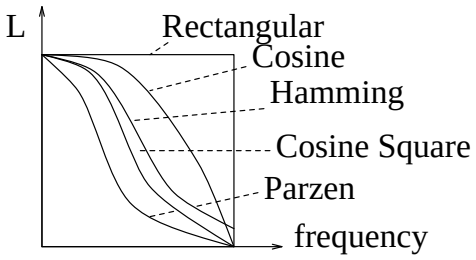

Figure 1: Different types of apodisation functions in the frequency domain.

5 A use of the GFBP and the LFBP operators

We have now three basic procedures FBP, GFBP and LFBP which give respectively the absorption coefficient, the gradient vector and the laplacien value for any point in the slice with reel coordinates. Figure 2 is the reconstructed image of a slice at the level of the ears with conventional FBP (real data). Figure 3 is a zoom ($\times 5$) performed on this image, simply by using the FBP operator with a thinner grid (it is unusual to zoom that much when reconstructing the image). Figure 4 represents the image of the norm of the gradient, obtained with the GFBP operator and figure 5 is a binary image representing the sign of the laplacien obtained with the LFBP. We compare also the laplacien computed with a conventional method (figure 6, $\sigma = 1.5$), with the result of our method, with a cosine square apodisation (figure 7).

Let us see now a way to use those procedures to find the boundaries of an object, without computing a digital image of the slice. The example presented here is very straightforward, but many other algorithms can be designed, like the use of deformable models.

Here we propose to simply find the zero-crossing of the laplacien by considering it to be the iso-contour 0 of the image of the laplacien. Methods to reconstruct iso-contours in 3D images, with some guaranties about the topological properties of those surfaces are described in [13] or in [10]. The restriction of these algorithms to 2D images leads also to reconstructed iso-contours which are continuous closed curves (except for the image boundaries), despite that the computation is independent from one pixel to another

one. The position of the contour is adjusted to sub-pixel values with linear interpolation along the sides of the pixels (see [10] for implementation details of the algorithm).

The laplacien do not suffice to segment the image, because it can perform only the *localization* of the contours, and not their *detection*. In other words, there will be zero-crossing at the boundaries of the objects, but also in part of the image with almost constant intensity, because of the noise (see figure 8). We chosed to track only the zero-crossing corresponding to high values of the gradient norm, which explaines why both the GFBP and LFBP operators were needed.

If we compute all the contours corresponding to a grid of a fixed resolution, say $n \times n$ pixels, and if p is the number of projection and q the number of detectors in the sinogram, if K is the size in pixels of the support of the convolution filter for the computation of the filtered sinogram, the complexity of our method is the following:

- $o(pqK)$ for the pre-computation of the filtered sinogram.
- $o(pn^2)$ for the edge extraction.

K is generally a small fixed number, and p and q are of the same order than n. The complexity can be roughly approximated with $o(n^2)$ for the pre-computation, and $o(n^3)$ for the edge extraction. In that case, we have computed the entire image of the laplacien and of the gradient, which reduce the advantage of getting rid of the computation of the absorption coefficient image (whose complexity is also $o(n^3)$).

What we claim is that there is no need to compute so many values to extract the main boundaries of the image. In the following experiment, we started with randomly distributed "seeds" in the plane of the slice. A "seed" is a pixel of the grid, for which we test if a contour is coming through. In that case, we follow and extract the contour, until the edge of the slice is reached, or the contour is closed, or also if the gradient norm is bellow a given threshold (this algorithm is the reduction to 2D of a similar algorithm described in [10] for the 3D case). For real experiments, we observed that with only very few seeds, the main contours are extracted.

A numerical example helps to understand this: the probability $P_{miss}(r, s)$ of missing a contour that goes through r pixels with s seeds in a $n \times n$ grid

is $(1 - r/n^2)^s$. If we say that a contour is significant if its length is at least $r > n$, and if we choose to take $s = nk$ seeds, then $P_{miss}(n, kn)$ is swiftly equivalent to exp^{-k}. The complexity of the algorithm is $o(kn^2 + Rn)$, where R is the sum of the length of all the extracted contours. For example, for $k = 4$, $P_{miss}(n, 4n)$ is lesser than 2%; in other words, the algorithm used to extract contours of length greater than n pixels, out of a grid of n^2 pixels, with a probability of missing $P_{miss} < 0.02$ necessitates the computation of only $4n$ seeds, that is, $4/n$ times the total number of computations for the entire image, which gives an intuitive understanding of our assumption, and a way to evaluate the number of seeds s requested for a given application. Image 9 represent the extracted contours with $k = 30$ whereas figure 8 represent the all the zero crossings of the image (the resolution is $n = 512$). The number of GFBP and LFBP calls for the random algorithm is only one tenth of the number of calls to perform to reconstruct the gradient and laplacien images (GFBP calls: 23035, LFBP calls: 30324).

At last, our algorithm can be used with a single seed, to track a single contour. The algorithm of tracking a single contour whose length is of the order of n is therefore $o(n^2)$, which is a tradeoff between the algorithm in $o(n)$ that we proposed previously in [12] (which is faster but less robust), and the $o(n^3)$ required for the computation of the image of the slice in traditional methods. Image 10 is the example of such a tracking. Only one point of the contour has been specified, and the entire contour has been reconstructed with 75 less computation than requested for an image reconstruction, with the same resolution (GFBP calls: 2313, LFBP calls: 4624). Furthermore, if a greater resolution is requested, our algorithm is linear with the size of the edge of the image, and not its surface. To compute this contour at the resolution of the zoomed image, it tooks only 5 times more computations, whereas the number of pixel of such an image is multiplied by 25 !, and we can see on figure 9 that reconstructing the contour at this resolution is not meaningless.

As we said previously, more evoluted segmentation algorithms can take use of the GFBP and LFBP. For example, deformable models (or "snakes") are used to find a contour which minimizes both internal and external constraints. Those two types of constraints correspond respectively to the elasticity of the deformable model and to an attraction force toward the contour points (see Kass87). In our case, the external constraints can be computed with the GFBP, which gives the direction and magnitude of the force, and

the sign of the LFBP which gives the orientation of this vector.

6 A word about the accuracy of the reconstruction

The problem of establishing the theoretical accuracy of the reconstructed images has never been fully investigated, mainly because this accuracy is strongly dependent on the shape of the studied object. The theoretical accuracy "... depends largely on the smoothness of the picture" (Louis and Natterer, in [6]). It depends on the relative contrast between the object elements and also on the geometric features of the objects. Furthermore, high density objects create serious artefacts which deteriorate the quality of the reconstructed image. At last, a mathematical definition of the "accuracy" itself must be given, which depends on the field of application of the method. The method proposed by Srinivasa et al. [8], is mathematically equivalent to the traditional method, only the discretization of the problem is different, which leads to a surprisingly different results of segmentation. The authors were wary to leave the interpretation of the quality of the result to the reader, and are not able to tell whether or not their method is more precise than the traditional one. We have exactly the same problem, and moreover, our method being mathematically different than the traditional one, a fair comparison is more difficult to establish (what σ to use ?). A theoretical comparison of the accuracy of those methods is a very challenging issue.

7 Conclusion

To conclude, we have presented two new operators, the Laplacien (LFBP) and the Gradient (GFBP) Filtered Back Projection operators, which can be used to compute gradient and laplacien values at any point of the slice, without image reconstruction. This method can be extended to the computation of any differential of the image. We have shown also how those operators can be designed to take the noise into account, and how to use them to compute efficiently a segmentation of the image. The final algorithm of boundary extraction can be achieved with far less computation than with traditional

methods, especially for the tracking of a single boundary along the time, and with a precision which is at least equal to traditional methods. More work is still needed to state the exact theoretical accuracy of the reconstructed gradient and laplacien value with the GFBP and LFBP, versus a solution where an image of the absorption coefficient is computed first.

Acknowledgment

I wish to thank Jean-Marie Rocchisani and Nicholas Ayache for stimulating discussions about this subject, and also Mr Bertinati from Siemens France, who provided the sinogram of the head scan.

References

[1] John Canny. A computational approach to edge detection. *IEEE PAMI*, 8(6):679–698, November 1986.

[2] Rachid Deriche. Using Canny's criteria to derive a recursively implemented optimal edge detector. *International Journal of Computer Vision*, 6:167–187, November 1986.

[3] Budinger T.F. Gullberg G.T. The use of filtering methods to compensate for constant attenuation in single photon emission computed tomography. *IEEE Trans. Biom. Eng.*, BME 28(2):142–157, 1981.

[4] M. Jatteau and C. Berche. Review of image reconstruction techniques in medical transactial computed tomography. *Ann. Radiol.*, 26(1):13–22, 1983.

[5] Avinash C. Kak. Image reconstruction from projections. In Michael P. Ekstrom, editor, *Digital Image Processing Techniques*, chapter 4. Academic Press, 1984.

[6] K. Louis, Alfred and Frank Natterer. Mathematical problems of computarized tomography. *Proceedings of the IEEE*, 71(3):379–389, March 1983.

[7] D. Marr and E.C. Hildreth. Theory of edge detection. *Proc. Roy. Soc. Lond. B.*, 207:187–217, 1980.

[8] N. Srinivasa, K.R. Ramakrishnan, and K. Rajgopal. Detection of edges from projections. *IEEE Trans. on Medical Imaging*, 11(1):76–80, March 1992.

[9] Rowland S.W. Computer implementation of image reconstruction formulas. In Herman G.T., editor, *Image Reconstruction from Projections: Implementation and Application*, volume 32, pages 9–79. Topics in Applied Physics, Springer Verlag, 1979.

[10] J-P. Thirion and Gourdon A. The 3d marching lines algorithm and its application to crest lines extraction. Technical Report 1672, INRIA, May 1992.

[11] J-P. Thirion and N. Ayache. Procédé et dispositif d'aide à l'inspection d'un corps, notamment pour la tomographie. Patent, April 1991.

[12] Jean-Philippe Thirion. Segmentation of tomographic data without image reconstruction. *IEEE Trans. on Medical Imaging*, 11(1):102–110, March 1992.

[13] G. Wyvill, C. McPheeters, and C. Wyvill. Data structures for soft objects. *Visual Computer*, 2:227–234, 1986.